Dyes and Pigments 86 (2010) 166–173

Contents lists available at ScienceDirect

Dyes and Pigments

journal homepage: www.elsevier.com/locate/dyepig

Highly-efficiency red-emitting platinum (II) complexes containing 4′-diarylamino-1-phenylisoquinoline ligands in polymer light-emitting diodes: Synthesis, structure, photoelectron and electroluminescence

Zhengyong Hu [a], Yafei Wang [a], Danyan Shi [a], Hua Tan [a], Xiaoshuang Li [a], Lei Wang [c], Weiguo Zhu [a,b,*], Yong Cao [c]

[a] College of Chemistry, Xiangtan University, Xiangtan 411105, China
[b] Key Lab of Environment-Friendly Chemistry and Application in Ministry of Education, Xiangtan 411105, China
[c] Institute of Polymer Optoelectronics Materials and Devices, South China University of Technology, Guangzhou 510640, China

ARTICLE INFO

Article history:
Received 10 October 2009
Received in revised form
22 December 2009
Accepted 25 December 2009
Available online 6 January 2010

Keywords:
Platinum (II) complex
Synthesis
Electroluminescence
Photoluminescence
Phosphorescence
Polymer light-emitting devices

ABSTRACT

Heteroleptic cyclometalated platinum (II) complexes bearing diarylamino-functionalized 1-phenylisoquinoline derivatives as primary ligand and acetyl acetonate as ancillary ligand were prepared and characterized. Single-crystal X-ray diffraction revealed that platinum (II) (4-(isoquinolin-1-yl)-*N*,*N*-diphenylbenzenamine-N,$C^{2\prime}$) (2,4-pentanedionato-*O*,*O*) displayed square planar molecular geometry with Pt···Pt separation of 6.328 and 6.275 Å. The platinum (II) complexes displayed good thermal and morphological stability, as well as intense ligand-centered fluorescence and π–π^* phosphorescence at 298 K, as well as strong phosphorescence at 77 K in dichloromethane. The double-layer polymer light-emitting diodes using **6a** as emitters and a blend of poly(9,9-dioctylfluorene) and 2-(4-*tert*-butyl)-phenyl-5-biphenyl-1,3,4-oxadiazole as host matrix exhibit best performance with the maximum external quantum efficiency as high as 8.6% at 0.66 mA cm^{-2}.

1. Introduction

Phosphorescent cyclometalated platinum (II) complexes have attracted considerable interest in the context of their application in the fields of optical chemosensors [1–5], photocatalysts [6–8], solar energy conversion [9–11] and organic/polymer light-emitting diodes (OLEDs/PLEDs) [12–15]. As cyclometalated platinum complexes have strong spin–orbital coupling at room temperature and can use both singlet and triplet excitons to emit highly efficient-phosphorescence, they are often used as blue, green, red, near-infrared and white emittors in OLEDs/PLEDs of high emission efficiency [16–19]. A white-emitting OLED with external quantum efficiency (EQE) of 18.3% and a red/near-infrared OLED with an EQE up to 14.5% were reported by Massimo and Cocchi respectively [16,17].

Compared to iridium complexes, cyclometalated platinum complexes, however, display lower emission efficiency [20–22] because the planar molecules tend to aggregate, thereby resulting in pronounced triplet–triplet (T–T) annihilation; also, as the platinum (II) ion has a higher atomic number than both osmium (II) and iridium (III) ions, platinum (II) complexes generally display longer phosphorescence lifetime (~50 μs) and exhibit rapidly decreased emission efficiency at high current density.

To realize the commercial practical application of platinum (II) complexes in OLEDs/PLEDs, researchers have sought to reduce phosphorescent lifetime and prevent aggregation, thereby enhancing carrier-transporting properties. For example, Kavitha et al. reported a non-planar isoquinolinyl indazole-based cyclo-metalated platinum (II) complex, $Pt(iqdz)_2$ [19], in which a camphor-like structure was introduced in the cyclometalated ligand, which displayed high luminescent efficiency in OLED with a maximum EQE of 14.9% (24.57 cd A^{-1}) at 100 mA cm^{-2}. Wong and co-workers fabricated a multifunctional platinum complex by the covalent linkage of oxadiazole and triarylamine units with the cyclometalated ligand and reported its improved electron- and hole-transporting properties [23].

* Corresponding author at: College of Chemistry, Xiangtan University, Xiangtan 411105, China. Tel.: +86 731 58298280; fax: +86 731 58292251.
E-mail address: zhuwg18@126.com (W. Zhu).

0143-7208/$ – see front matter © 2009 Elsevier Ltd. All rights reserved.
doi:10.1016/j.dyepig.2009.12.014

Previous work by the current authors showed that the introduction of a diphenylamino group in the cyclometalated ligand provided a high-efficiency, green-emitting [*N*,*N*-diphenyl-4-(2′-pyridyl) aniline-C^3, N^1] (diphenoxylmethane) platinum (II) complex, [(PhNPPy)Pt(DBM)] [24]. This paper concerns red-emitting, phosphorescent, cyclometalated platinum (II) complexes, namely (Piq-G)Pt(acac), in which *Piq-G* is a 1-phenylisoquinoline derivative that contains diarylamino groups at the 4-position of the phenyl ring and *acac* is acetyl acetonate. As the Piq-G cyclometalated ligand has a non-planar, triphenylamino configuration and the triphenylamino group has excellent hole-transporting characteristic, the diarylamino-functionalized (Piq-G)Pt(acac) complexes are expected to display superior electroluminescence than the corresponding non-functionalized (Piq)Pt(acac) complex. Using (Piq-G)Pt(acac) rather than (Piq)Pt(acac) as emitter and a blend of poly(9,9-dioctylfluorene) (PFO) and 2-(4-*tert*-butyl)-phenyl-5-biphenyl-1,3,4-oxadiazole (PBD) as host matrix, fabricated double-layer, polymer light-emitting diodes exhibited bright red-emission at 641 ± 4 nm and displayed an EQE of 8.6%.

2. Experimental

2.1. Chemicals and instruments

All solvents were carefully dried and distilled prior to use. Commercially available reagents were used without further purification unless otherwise stated. All reactions were performed under nitrogen atmosphere and were monitored by thin-layer chromatography (TLC). Flash column chromatography and preparative TLC were carried out using silica gel from Merck (200–300 mesh). All ^{1}H NMR spectra were acquired at a Bruker Dex-400NMR instrument using $CDCl_3$ as a solvent. Elemental analysis was performed on a Harrios elemental analysis instrument.

2.2. Synthesis

2.2.1. 4-Nitro-N-phenethylbenzamide (**1**)

To a solution of 4-nitrobenzoyl chloride (31.5 g, 169 mmol) in 350 mL of methylene chloride was added dropwise β-phenethylamine (22.2 mL, 169 mmol) at 0 °C followed by an addition of triethylamine (26 mL, 169 mmol). The reaction mixture was then warmed to room temperature and stirred for 26 h after which time, the mixture was diluted with CH_2Cl_2 and neutralized with aq. $NaHCO_3$ solution. The organic phase was washed with aq. $NaHCO_3$ solution and brine, dried over anhydrous Na_2SO_4 and residue was purified by recrystallization from ethanol to form yellow coloured crystals of **1** (35.5 g, 88%). m.p. 125 °C. ^{1}H NMR (400 MHz, $CDCl_3$), ppm: 8.27 (d, 2H, J = 8.8 Hz), 7.85 (d, 2H, J = 8.8 Hz), 7.37 (dd, 2H, J = 7.2, 7.6 Hz), 7.28 (dd, 3H, J = 15.6, 7.2 Hz), 6.24 (s, 1H), 3.78 (ddd, 2H, J = 6.4, 6.4, 6.4 Hz), 2.98 (dd, 2H, J = 6.8, 6.8 Hz).

2.2.2. 1-(4-Nitrophenyl)-3, 4-dihydroisoquinoline (**2**)

To a solution of **1** (35.5 g, 0.13 mol) in 54 mL of xylene was added P_2O_5 (caution: incompatible with sodium, aluminum, potassium, ammonia, peroxides and magnesium; reacts violently with water; hazardous Decomposition Products; 37 g, 0.13 mol) and 103 mL of $POCl_3$ (caution: extremely reactive or incompatible with acids; highly reactive with reducing agents, combustible materials, organic materials, metals, alkalis, moisture; may undergo hazardous decomposition, condensation or polymerization) with stirring. The mixture was refluxed for 5 h and the concentrated residue was carefully neutralized with 10% aq. sodium hydroxide solution. The mixture was extracted with CH_2Cl_2., the organic layer being dried over anhydrous magnesium sulfate and evaporated to provide a brown-yellow solid (22.7 g, 69%). m.p. 88 °C. ^{1}H NMR (400 MHz, $CDCl_3$), ppm: 8.26 (d, 2H, J = 8.4 Hz), 7.76 (d, 2H, J = 8.4 Hz), 7.41 (dd, 1H, J = 7.2, 7.6 Hz), 7.28 (dd, 2H, J = 16.8, 7.6 Hz), 3.88 (dd, 2H, J = 7.2, 7.6 Hz), 2.81 (dd, 2H, J = 7.6, 7.2 Hz).

2.2.3. 1-(4-Nitrophenyl)isoquinoline (**3**)

A mixture of **2** (13.9 g, 0.055 mol) and 1.18 g of 10% Pd/C in 250 mL of 1, 2, 3, 4-tetrahydronaphthalene was refluxed under nitrogen for 15 h. The catalyst was removed from the hot mixture by filtration and tetrahydronaphthalene was removed under vacuum. The residue was dissolved in concentrated hydrochloric acid and filtered, the filtrate being carefully neutralized with aq. sodium hydroxide solution. The precipitate was extracted with CH_2Cl_2. and the organic layer was dried over anhydrous magnesium sulfate and evaporated to afford a yellow solid (9.8 g, 73.1%). m.p. 96 °C. ^{1}H NMR (400 MHz, $CDCl_3$), ppm: 8.58 (d, 1H, J = 5.6 Hz), 8.22 (d, 1H, J = 8.4 Hz), 7.87 (d, 1H, J = 8.0 Hz), 7.69 (dd, 1H, J = 7.2, 8.0 Hz), 7.59 (m, 4H), 6.85 (d, 2H, J = 8.0 Hz).

2.2.4. 4-(Isoquinolin-1-yl)benzenamine (**4**)

A mixture of **3** (9.8 g, 39.2 mmol) and 170 mL of ethanol was heated to 50 °C followed by the addition of 0.392 g of 5% Pd/C. A further 0.392 g of 5% Pd/C and 9 mL of 80% hydrazine hydrate (caution: incompatible with oxidizing agents, heavy metal oxides, dehydrating agents, alkali metals, rust, silver salts; combustible; contact with many materials may cause fire or explosive decomposition; may react explosively with a variety of materials; vapour may explode in fire) were added over 40 min. The ensuing mixture was refluxed for 4 h after which time, the catalyst was removed from the hot solution by filtration. The filtrate was evaporated to remove the majority of ethanol and mixed with water; the yellow solid was realized by filtration (8.1 g, 93.6%). m.p. 197–199 °C. ^{1}H NMR (400 MHz, $CDCl_3$), ppm: 8.58 (d, 1H, J = 5.6 Hz), 8.22 (d, 1H, J = 8.4 Hz), 7.87 (d, 1H, J = 8.0 Hz), 7.69 (dd, 1H, J = 7.2, 8.0 Hz), 7.59 (m, 4H), 6.85 (d, 2H, J = 8.0 Hz), 3.88 (s, 2H).

2.2.5. 4-(Isoquinolin-1-yl)-N,N-diphenylbenzenamine (**5a**)

A mixture of **4** (1.3 g, 5.9 mmol), iodobenzene (1.7 mL, 14.5 mmol), anhydrous K_2CO_3 (6.6 g, 47.8 mmol), 1.5 g bronze powder, 0.4 g of dibenzo-18-crown-6 and 25 mL 1,2-dichlorobenzene was refluxed under nitrogen for 24 h and cooled to room temperature. The reaction mixture was filtered to remove the precipitated base and evaporated under reduced pressure to remove solvent. The resulting brown-yellow oily crude was purified by silica gel column chromatography using dichloromethane/hexane (1:20, v/v) as eluent provide a yellow solid (1.7 g, 77.6%). m.p. 142–144 °C. ^{1}H NMR (400 MHz, $CDCl_3$), ppm: 8.60 (d, 1H, J = 5.6 Hz), 8.26 (d, 1H, J = 8.4 Hz), 7.9 (d, 1H, J = 8.4 Hz), 7.73 (dd, 1H, J = 7.2, 7.6 Hz), 7.64 (m, 4H), 7.32 (dd, 3H, J = 8.4, 7.2 Hz), 7.23 (dd, 6H, J = 8.8, 8.4 Hz), 7.08 (dd, 3H, J = 7.2, 7.2 Hz).

2.2.6. 4-(Isoquinolin-1-yl)-N,N-dip-tolylbenzenamine (**5b**)

The synthesis described for **5a** was followed. A yellow solid **5b** was obtained in 72.3% yield. m.p. 153–155 °C. ^{1}H NMR (400 MHz, $CDCl_3$), ppm: 8.58 (d, 1H, J = 6.0 Hz), 8.25 (d, 1H, J = 8.4 Hz), 7.88 (d, 1H, J = 8.4 Hz), 7.70 (dd, 1H, J = 7.2, 7.2 Hz), 7.60 (m, 4H), 7.17 (d, 2H, J = 8.4 Hz), 7.12 (m, 8H), 2.33 (s, 6H).

2.2.7. 4-Tert-butyl-N-(4-tert-butylphenyl)-N-(4-(isoquinolin-1-yl) phenyl)benzenamine (**5c**)

The synthesis described for **5a** was followed. A yellow solid **5c** was obtained in 62.9% yield. m.p. 186–188 °C. ^{1}H NMR (400 MHz, $CDCl_3$), ppm: 8.59 (d, 1H, J = 6.0 Hz), 8.27 (d, 1H, J = 8.4 Hz), 7.89 (d, 1H, J = 8.0 Hz), 7.72 (dd, 1H, J = 7.2, 7.2 Hz), 7.62 (m, 4H), 7.31 (d, 4H, J = 8.8 Hz), 7.21 (d, 2H, 8.4 Hz), 7.13 (d, 4H, J = 8.4 Hz), 1.33 (s, 18 H).

*2.2.8. Platinum (II) (4-(isoquinolin-1-yl)-N,N-diphenylbenzenamine-N, $C^{2\prime}$) (2,4-pentane dionato-O,O) (**6a**)*

A mixture of **5a** (0.7 g, 1.88 mmol) and K_2PtCl_4 (0.39 g, 0.94 mmol) was stirred in 2-ethoxyethanol (20 mL) and water (7 mL), and was then heated to 80 °C for 16 h. After cooling to room temperature, the mixture was added to water (20 mL) and the resulting precipitate was collected and washed with water (20 mL × 4) to provide the partial dimmer. The dimer (400 mg, 0.33 mmol), acetylacetone (83 mg, 0.83 mmol) and Na_2CO_3 (280 mg, 2.64 mmol) were mixed in 2-ethoxyethanol (30 mL) and the mixture was stirred at 100 °C for 24 h. The solvent was then removed under reduced pressure, and the residue was purified by flash chromatography using dichloromethane as the eluent to provide **6a**. The **6a** product was then recrystallized with dichloromethane/hexane to afford red crystal with an isolated yield of 30.5% (135 mg, 0.05 mmol). m.p. 222–225 °C. ^{1}H NMR (400 MHz, $CDCl_3$), ppm: 8.84 (ddd, 2H, J = 6.8, 4.4, 8.8 Hz), 7.94 (d, 1H, J = 8.8 Hz), 7.80 (d, 1H, J = 8.0 Hz), 7.71 (dd, 1H, J = 6.8, 7.6 Hz), 7.61 (dd, 1H, J = 7.2, 7.6 Hz), 7.33 (m, 10H), 7.10 (dd, 2H, J = 7.2, 6.8 Hz), 6.82 (ddd, 1H, J = 2.4, 6.4, 2.4 Hz), 5.39 (s, 1H), 1.9 (s, 3H), 1.7 (s, 3H). Anal. calcd for $C_{32}H_{26}N_2O_2Pt$: C, 57.74; H, 3.94; N, 4.12. found: C, 57.44; H, 3.90; N, 4.15.

*2.2.9. Platinum (II)(4-(isoquinolin-1-yl)-N,N-di-p-tolylbenzenamine-N,$C^{2\prime}$)(2,4-pentanedionato-O,O)(**6b**)*

The synthesis of **6a** was followed to realize the red solid **6b** in 27.6% yield. m.p. 262–263 °C. ^{1}H NMR (400 MHz, $CDCl_3$), ppm: 8.81 (dd, 2H, J = 6.4, 8.8 Hz), 7.89 (d, 1H, J = 8.4 Hz), 7.79 (d, 1H, J = 7.6 Hz), 7.70 (dd, 1H, J = 7.2, 8.4 Hz), 7.59 (dd, 1H, J = 8.4, 7.6 Hz), 7.16 (ddd, 10H, J = 8.4, 7.6, 8.4 Hz), 6.77 (ddd, 1H, J = 2.4, 6.4, 2.4 Hz), 5.39 (s, 1H), 2.33 (s, 6H), 1.99 (s, 3H), 1.70 (s, 3H). Anal. calcd for $C_{34}H_{30}N_2O_2Pt$: C, 58.87; H, 4.36; N, 4.04. found: C, 58.90; H, 4.52; N, 4.01.

*2.2.10. Platinum (II) (4-tert-butyl-N-(4-tert-butylphenyl)-N-(4-(isoquinolin-1-yl)phenyl) benzeneamine-N, $C^{2\prime}$) (2,4-pentanedionato-O,O) (**6c**)*

The synthesis of **6a** was followed to realize the red solid **6c** in 33.9% yield. m.p. 266–268 °C. ^{1}H NMR (400 MHz, $CDCl_3$), ppm: 8.81 (dd, 2H, J = 2.8, 5.2 Hz), 7.91 (d, 1H, J = 8.8 Hz), 7.79 (d, 1H, 8.0 Hz), 7.71 (ddd, 1H, J = 5.2, 6.0, 8.0 Hz), 7.58 (dd, 1H, J = 7.6, 8.0 Hz), 7.33 (d, 5H, J = 8.8 Hz), 7.20 (d, 5H, J = 8.4 Hz), 6.78 (d, 1H, J = 6.8 Hz), 5.38 (s, 1H), 1.99 (s, 3H), 1.68 (s, 3H), 1.32 (s, 18H). Anal. calcd for $C_{40}H_{42}N_2O_2Pt$: C, 61.76; H, 5.44; N, 3.60. found: C, 61.43; H, 5.50; N, 3.57.

*2.2.11. Platinum (II)(1-phenylisoquinoline-N,$C^{2\prime}$) (2,4-pentanedionato-O,O) (**piq)Pt(acac**)*

The synthesis of **6a** was followed to realize the red solid **6b (piq) Pt(acac)** in 38.9% yield. m.p. 184–186 °C. ^{1}H NMR (400 MHz, $CDCl_3$), ppm: 8.99 (d, 1H, J = 6.4 Hz), 8.92 (d, 1H, J = 8.0 Hz), 8.11 (d, 1H, J = 6.8 Hz), 7.86 (d, 1H, J = 8.4), 7.79 (m, 2H), 7.69 (dd, 1H, J = 8.0, 7.6 Hz), 7.45 (d, 1H, J = 6.0 Hz), 7.28 (m, 3H), 5.49 (s, 1H), 2.04 (d, 6H, 3.2 Hz). Anal. calcd for $C_{20}H_{17}NO_2Pt$: C, 48.18; H, 3.44; N, 2.81. found: C, 48.32; H, 3.52; N, 2.78.

2.3. Physical measurement

Thermo-gravimetric analysis (TGA) was carried out with a NETZSCH STA449 from 25 to 700 °C at a heating rate of 20 °C/min under nitrogen. UV–vis absorption spectra were recorded on a PerkinElmer Lambda 25 UV–vis absorption spectrophotometer. Photo-luminescence (PL) spectra were recorded with an Insta-Spec IV CCD system (Oriel) under excitation of 325 nm line of a He–Cd laser (OmniChrome Co.). Photoluminescent lifetimes of the iridium complexes in their doped films were probed at the emission peak of 610 nm on the Edinburgh FLS920 system under excitation of 230 nm line of hydrogen laser. The iridium complexes-doped films have a thickness of 80 nm and a 4% dopant concentration.

2.4. X-ray diffraction studies

Good-quality crystals of **6a** were grown from chloroform/hexane solution at room temperature. Single-crystal X-ray diffraction data were measured on a Bruker SMART Apex CCD diffractometer using μ(Mo Kα) radiation (λ = 0.71073 Å). The data collection was executed using an SMART program. Cell refinement and data reduction were performed by a SAINT program. The structure was determined using an SHELXTL/PC program and refined using full-matrix least squares. Crystallographic refinement parameters of complexes **6a** and their selective bond distances and angles are summarized in Table 1 and Fig. 1, respectively.

2.5. Electrochemical measurements

Electrochemical measurements were made using a CHI660A electrochemical work station. A conventional three-electrode configuration consisting of a Pt working electrode, a Pt-wire counter electrode and a calomel electrode reference electrode was used. The solvent in all measurements was CH_3CN, and the supporting electrolyte was 0.1 M $[Bu_4N]PF_6$. Ferrocene was added as a calibrant after each set of measurements, and all potentials reported were quoted with reference to the ferrocene/ferrocenium (Fc/Fc^+) couple at a scan rate of 50 mV s^{-1}.

2.6. Device fabrication and characterization

The host material of PFO was purchased from American Dye Sources Inc. Polyvinylcarbazde (PVK) and PBD was purchased from Aldrich. Poly(ethylenedioxythiophene):poly(styrene sulfonic acid) (PEDOT:PSS, Baytron P 4083, purchased from Bayer AG). Device configuration is ITO/PEDOT (50 nm)/(PVK) (50 nm)/Pt(II) complexes (*x*%) + PFO:PBD [80:20] (75 nm)/Ba (4.5 nm)/Al (150 nm) (Fig. 4, inset).

The fabrication of electrophosphorescent devices was carried out by following the standard procedure. A 50 nm of PEDOT : PSS

Table 1
Crystal data and refinement parameters for the **6a** complex.

	6a
Formula	$C_{64}H_{54}N_4O_4Pt_2$
Crystal size (mm)	0.30 × 0.12 × 0.08
Molecular mass	1333.29
Crystal system	Triclinic
Space group	$P_{\bar{1}}$
a (Å)	10.2132 (2)
b (Å)	10.4580 (2)
c (Å)	24.967 (4)
α (°)	80.173 (8)
β (°)	81.232 (8)
γ (°)	68.898 (8)
V (Å^3)	2439.3 (7)
Z	2
T (K)	173 (2)
D_{calc} (g cm^{-3})	1.815
F (000)	1308
Reflections collected	18154
Independent reflections	8306
Data/re strain/parameters	8306/0/671
Goodness-of-fit on F^2	1.124
Final R indices [I > 2r(I)]	R_1 = 0.0582, wR_2 = 0.1102
R indices (all data)	R_1 = 0.0894, wR_2 = 0.1228

$R_1 = \Sigma(|Fo|-|Fc|)/\Sigma|Fo|$; $wR_2 = [\Sigma w(Fo^2 - Fc^2)^2/\Sigma w(Fo^2)^2]^{1/2}$.

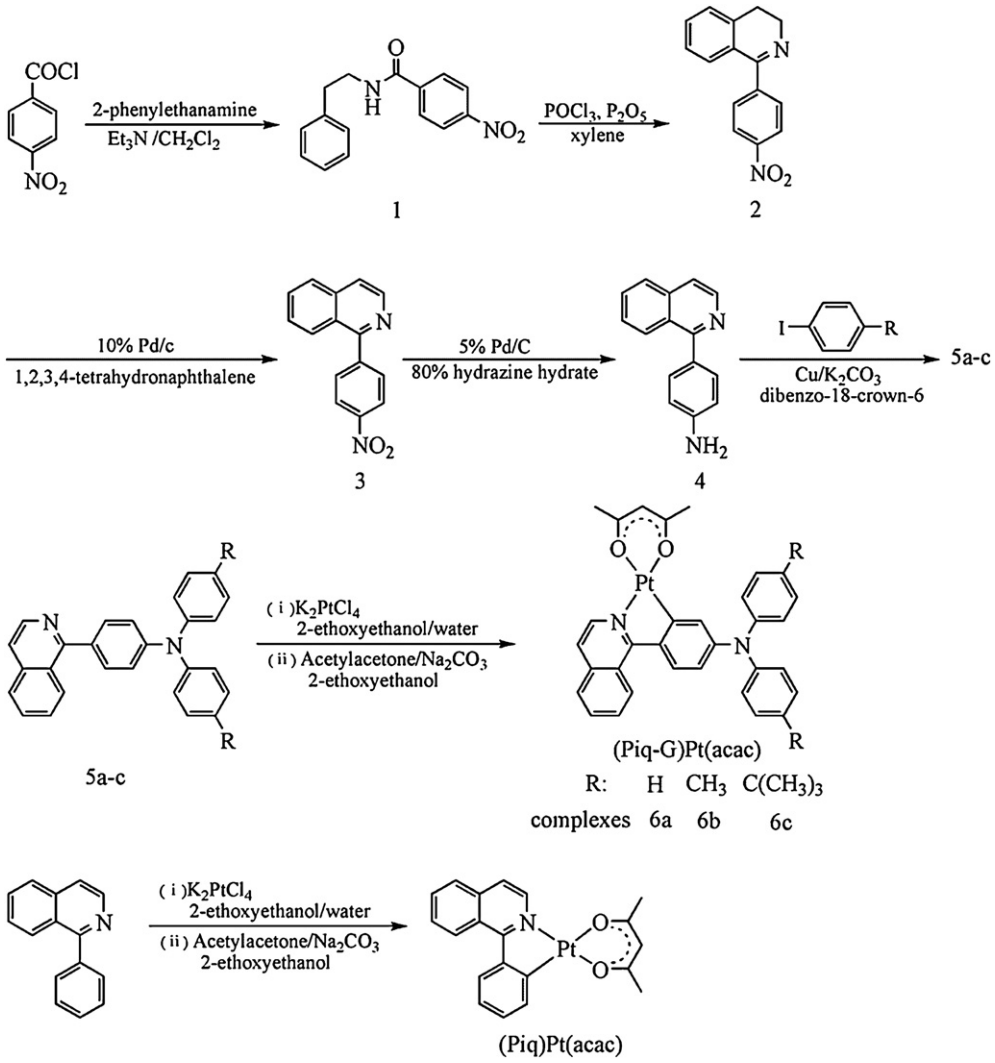

Fig. 1. Synthetic route for the (Piq-G)Pt(acac) and (Piq)Pt(acac) complexes.

was fistly spin-casted onto pre-cleaned ITO-glass substrates, a 50 nm of PVK was spin-casted on the top of PEDOT, and a 75 nm of emitting layer containing the platinum complex, PFO and PBD was spin-casted on the top of PVK. Finally, a 5 nm of Ba and 150 nm of Al were deposited on the top of the emitting layer successfully.

A profilometer (Tencor Alfa-Step 500) was used to determine the thickness of the spin-casted films. Layer thickness of thermal deposition was monitored by a crystal thickness monitor (Sycon). Current density (I)–voltage (V) data were collected using a Keithley 236 source measurement unit External quantum efficiencies (EQE) were obtained by measuring the total light output in all directions in an integrating sphere (IS-080, Labsphere). The luminance was measured by a Si photodiode, and calibrated by using a PR-705 Spectrascan spectrophotometer (Photo Research). Electroluminescence (EL) spectra were recorded using a CCD spectrophotometer (Instaspec 4, Oriel).

3. Results and discussion

3.1. Synthesis of ligands and their platinum complexes

Fig. 1 shows the synthetic route of the diarylamino-functionalized cyclometalated ligands and their platinum (II) complexes. The cyclo-metalated ligand of 1-phenylisoquinoline (piq) and the intermediate of 4-(isoquinolin-1-yl) benzenamine were synthesized according to the literature [25]. 4′-diarylamino-1-phenylisoquinoline (Piq-G) was synthesized according to traditional Ullmann reaction [26]. All of these cyclometalated platinum (II) complexes were synthesized by two steps which contain a cyclometalation of K_2PtCl_4 with these cyclometalated ligands and a chloride cleavage of the resulting chloro-bridged dimmers with an ancillary ligand of pentane-2, 4-dione (Hacac) in the presence of a base [27]. Each of the **6a**–**c** complexes were purified by silica chromatography and characterized by ^{1}H NMR and elemental analysis to confirm their well-defined chemical structures.

3.2. Crystal structure of the *6a* complex

X-ray diffraction study reveals that the **6a** complex has two crystallographically independent platinum (II) atoms, two 4-(isoquinolin-1-yl)-*N*,*N*-diphenylbenzenamine (**5a**) and two acetylacetone. Two platinum (II) atoms are four-coordinated with the same square-planar coordination geometry. As shown in Fig. 2, Pt(1) and Pt(2) are coordinated by two oxygen atoms from acetylacetone ligand and one nitrogen and carbon atom from **5a** ligand. The Pt–O distances are in the ranges of 1.969 (7)–2.073 (5) Å, Pt–N distances

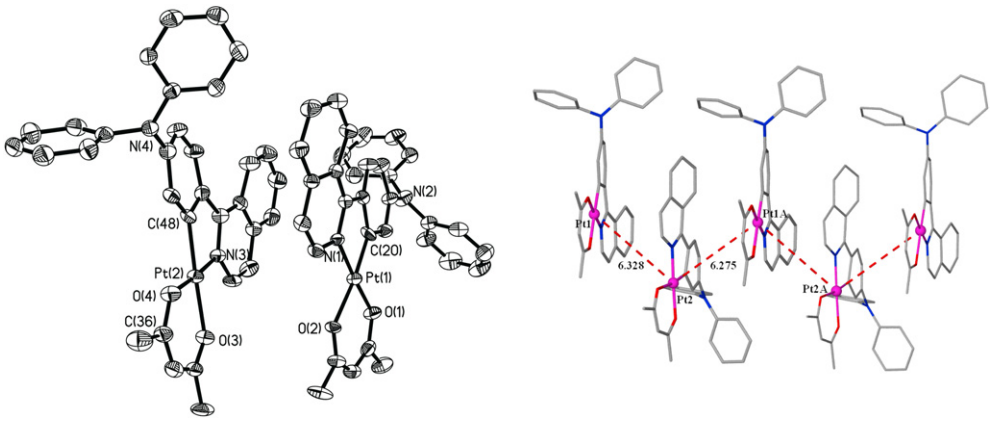

Fig. 2. ORTEP drawing of the complex 6a with thermal ellipsoids at 30% (all H atoms were omitted for clarity) and the Pt···Pt interactions in complex **6a**.

are 1.946 (7) Å and 1.964 (8) Å and Pt–C distances are 1.853 (9) Å and 1.933 (9) Å, while the bond angles for O–Pt–O are 90.5(3) and 91.6(3)° and for C–Pt–N are 80.3 (4) and 81.0 (4)°, respectively. Another interesting feature of complex **6a** is that two terminal isoquinoline rings from closest molecules are linked through face to face π-interactions. The isoquinoline groups of **5a** ligands are almost parallel and separated by a distance of about 3.5 Å. In the complex **6a**, the Pt&tnqh_8729;&tnqh_8729;&tnqh_8729;Pt distances are 6.328 and 6.275 Å, which is much longer than the reported Pt–Pt separation in the dimers of cyclometalated platinum (II) complexes (3.15–3.76 Å) [28,29]. The crystal data and refinement parameters are listed in Table 1.

3.3. Thermal and photophysical properties

The thermal properties of the (Piq-G)Pt(acac) complexes were examined by thermo-gravimetric analysis (TGA). All of the platinum (II) complexes generally exhibited high thermal stability and their onset decomposition temperature (T_d) ranged from 290 to 315 °C.

The absorption and emission spectra of the (Piq-G)Pt(acac) complexes in CH_2Cl_2 are shown in Fig. 3 and the data are summarized in Table 2. Two distinct high-energy absorption peaks at 300 and 390 nm (ε = 10 000–28 000 M^{-1} cm^{-1}), as well as one low-energy absorption peak at 480 ± 4 nm (ε = 5000–20 000 M^{-1} cm^{-1}), were observed for the (Piq-G)Pt(acac) complexes, in which the former high-energy bands are attributed to the cyclometalated

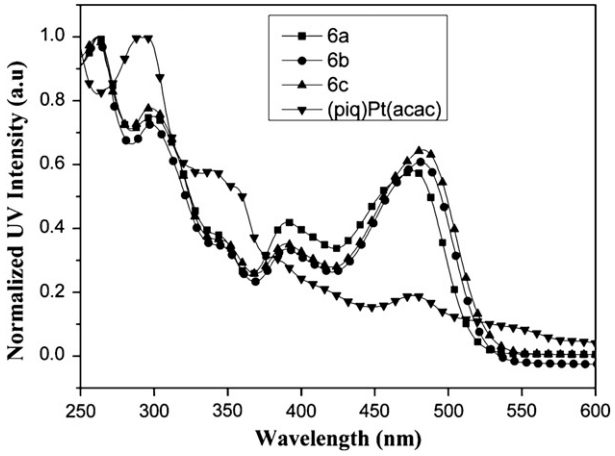

Fig. 3. Absorption spectra of platinum complexes in CH_2Cl_2 (1×10^{-5} M) at 298 K.

ligands-centered (LC) π–π* electron transitions and the latter low-energy bands are assigned to the metal-to-ligand charge transfer (MLCT) transitions resulting from strong spin–orbit coupling of these platinum complexes [30–34]. In these distinct absorption peaks, the low-lying absorption peak has slightly red-shift from 476 nm for R = H and 483 nm for R = Me due to different electron-donating effect of substituted group. As the introduction of an electron-releasing diarylamino group into the electron-deficient isoquinoline moiety is expected to increase the donor–acceptor (D–A) character of the cyclometalated ligand of piq-G, its (Piq-G)Pt (acac) complexes displayed larger low-lying MLCT absorption band than (Piq)Pt(acac) at about 480 nm, owing to a larger π-conjugation space and/or strong intramolecular D–A interaction, It is suggested that the enhanced MLCT absorption is useful to improve energy transfer from the host to the (Piq-G)Pt(acac) guest.

As revealed in Fig. 4b, the (Piq-G)Pt(acac) complexes in CH_2Cl_2 presented intense dual emission peaks at room temperature (298 K). The high-lying emission peak at 554 ± 11 nm is assigned to the ligand-centered $S_1 \rightarrow S_0$ relaxation (i.e., fluorescence), the other low-lying emission peak at 637 ± 2 nm is attributed to the ligand-centered $T_1 \rightarrow S_0$ transfer (i.e., phosphorescence) [35,36]. As a non-planar diarylamino group is introduced into the cyclometalated ligand of 1-phenylisoquinoline ligand, the platinum (II) center should occur a reduced spin–orbit interaction. Accordingly, both ligand-centered fluorescence and phosphorescence, and no MLCT emission were observed [37]. The substituent group has a significant effect on the high-and low-lying emission bands from the (Piq-G)Pt(acac) complexes. The high-lying emission peak was obviously red-shifted from 542 nm for R = H and 566 nm for R = Me. Using $(Piq)_2Ir(acac)$ as the standard (Φ = 0.20), the **6a**, **6b**, **6c** and (Piq)Pt(acac) complexes gave an emission quantum yields of 1.9%, 2.3%, 1.7% and 0.09% in CH_2Cl_2, respectively [38]. The (Piq-G)Pt (acac) complexes displayed 20 times fluorescence quantum

Table 2
Photophysical data for the (Piq-G)Pt(acac) and (Piq)Pt(acac) complexes.

Complex	T_d (°C)	λ_{abs}^{max} (ε, M^{-1} cm^{-1})	$\lambda_{em/nm}$			
			CH_2C1_2 (77 K)	CH_2Cl_2 (298 K)	Φ (%)	τ (μs)
6a	290	262 (20562), 301 (16237), 389 (9299), 477 (14176)	639, 698	543, 635	1.9	6.3
6b	306	262 (28248), 299 (22675), 389 (11139), 481 (20945)	647, 685	565, 637	2.3	6.5
6c	302	261 (23114), 299 (18666), 389 (8858), 483 (17511)	648, 704	565, 638	1.7	5.4
(Piq)Pt (acac)	315	290 (27000), 476 (5079)	591, 643	597, 639	0.9	3.5

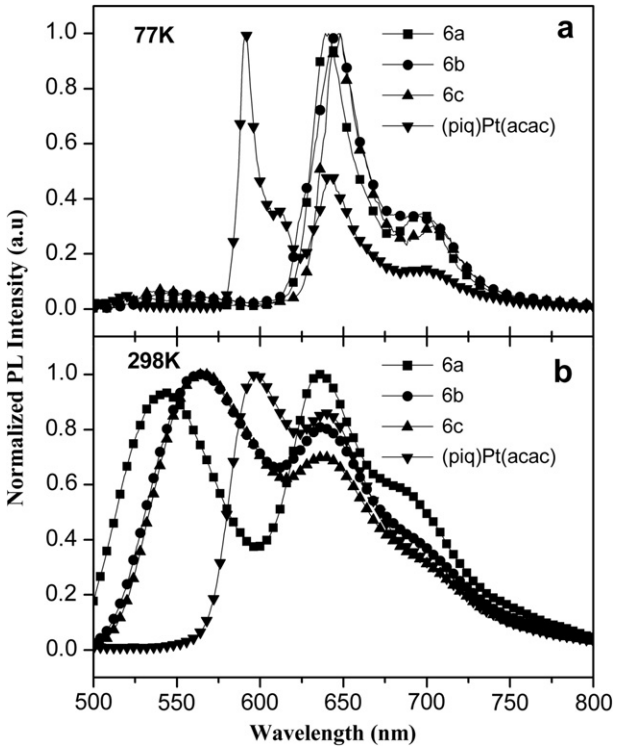

Fig. 4. Photoluminescence spectra for platinum complexes in CH_2Cl_2 at 298 K and 77 K under excitation of 476 nm light.

efficiency higher than (piq)Pt(acac). For comparision, low-temperature emission spectra were also recorded for the (Piq-G)Pt(acac) complexes at 77 K in Fig. 4a. Only one PL peak at 643 ± 5 nm with a shoulder at 695 ± 10 nm was observed in froze CH_2Cl_2, which is dominated by the intense MLCT phosphorescence. The ligand-centered $S_1 \rightarrow S_0$ emission bands of the **6a**–**c** complexes disappeared. This implies that an introduction of the bulky diarylamino group into cyclometalated ligand can significantly infect the emission character and efficiency of its platinum complexes.

3.4. Electrochemical property

The electrochemical properties of these diarylamino-functionalized platinum (II) complexes were examined using cyclic voltammetry and the corresponding data are listed in Table 3. Each of the (Piq-G)Pt(acac) complexes presented a reversible oxidation potential in a range of 0.69–0.72 V (vs. Fc/Fc^+), which is assigned to the oxidation of the triphenylamine moiety [37]. The reduction potentials were estimated based on the UV–vis absorption spectral edge (MLCT) and oxidation potential. The highest occupied molecular orbital (HOMO) and the lowest unoccupied molecular orbital (LUMO) energy levels of these platinum (II) complexes were then calculated according to an empirical formula using the Fc

Table 3
Electrochemical properties of the (Piq-G)Pt(acac) and (Piq)Pt(acac) complexes.

Complex	E_g (eV)	$E^{ox}_{1/2}$ (V)[a]	E^{red} (V)[a,b]	HOMO (eV)	LUMO (eV)	T1 (eV)
6a	2.39	0.69, 1.11	–	−5.49	−3.10	1.94
6b	2.36	0.72, 1.09	–	−5.52	−3.16	1.92
6c	2.36	0.72, 1.20	–	−5.52	−3.16	1.91
(Piq)Pt(acac)	2.48	–	1.57	−5.71	−3.23	2.09

[a] 0.1 M $[Bu_4N]PF_6$ in CH_3CN, scan rate 50 mV s^{-1}, vs. Fc/Fc^+ couple.
[b] Irreversible wave.

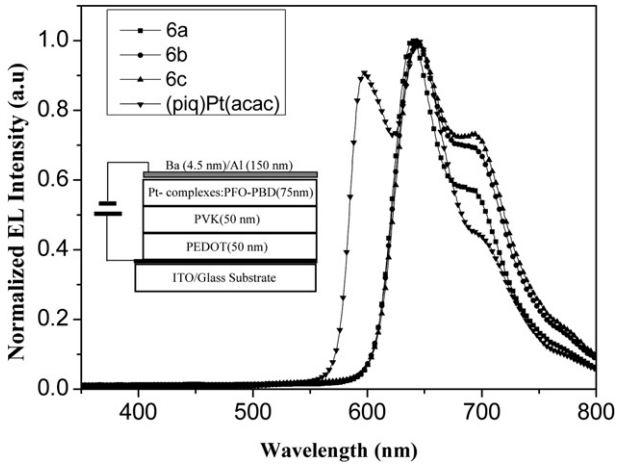

Fig. 5. Electroluminescence spectra for the platinum complexes-doped PLEDs (inset: the configuration of the PLEDs).

value of 4.8 eV below the vacuum level [39]. The calculated HOMO and LUMO energy levels for these Pt(II) complexes were −5.52 to 5.49 eV and −3.10 to 3.16 eV, respectively, which match closely with the energy levels for PFO (HOMO: −5.8 eV, LUMO: −2.1 eV) and PBD (HOMO: −6.2 eV, LUMO: −2.6 eV). The HOMO energy levels of the **6a**, **6b**, **6c** and (Piq)Pt(acac) were −5.49, −5.52, −5.52 eV and −5.71 eV respectively. Compared to the (Piq)Pt(acac) complex, the (Piq-G)Pt(acac) complexes displayed significantly increased HOMO level. This indicates that incorporation of the electron-rich diarylamino moiety into platinum complexes can effectively raise the HOMO energy level and improve the hole-transporting property of the platinum complexes.

3.5. Electroluminescent properties

To illustrate the electrophosphorescent performance of these platinum complexes, the double-layer PLEDs were fabricated by employing these platinum (II) complexes as emitting guests and a blend of PFO and PBD as a host matrix. Their electroluminescence (EL) spectra are shown in Fig. 5. Only one EL band peaked at 639–700 nm was observed for each of these devices at different dopant concentrations. The emission from PFO-PBD was not observed in all cases, even at high current densities and at low dopant concentration less than 1% (w/w). As the triplet energy levels of the (Piq-G)Pt(acac) complexes are calculated to be 1.88–2.09 eV

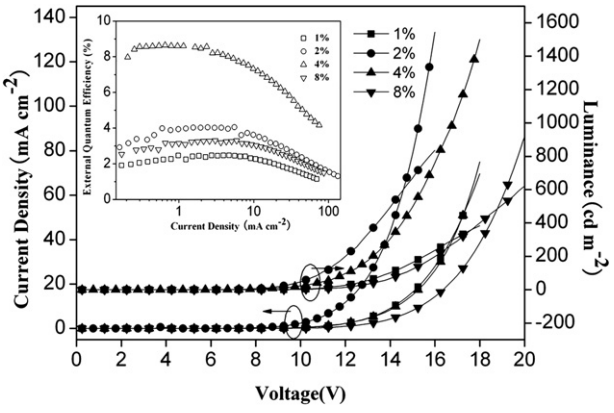

Fig. 6. Current density–voltage–luminance (*I*–*V*–*L*) curves of the **6a**-doped PLEDs at different doping concentrations.

Table 4
Device performances of the (Piq-G)Pt(acac)- and (Piq)Pt(acac)-doped PLEDs.

Pt complexes	Dopant ratio (wt%)	*V* turn-on (V)	*L* (cd m^{-2})	EQE_{max} (%)	LE_{max} (cd A^{-1})	λ_{max} (nm)	CIE
6a	1%	8	383 (69.77 mA/cm^2)	2.47 (4.70 mA/cm^2)	1.19	639, 687	0.66, 0.31
	2%	6	836 (133.34 mA/cm^2)	4.04 (5.53 mA/cm^2)	1.94	637, 684	0.67, 0.31
	4%	5.5	1501 (75.03 mA/cm^2)	8.64 (0.66 mA/cm^2)	4.15	639, 697	0.66, 0.30
	8%	8	622 (86.65 mA/cm^2)	3.30 (5.92 mA/cm^2)	1.58	639, 686	0.66, 0.31
6b	1%	6	541 (126.33 mA/cm^2)	1.95 (11.45 mA/cm^2)	0.87	643, 698	0.66, 0.31
	2%	6.5	596 (91.43 mA/cm^2)	4.12 (2.63 mA/cm^2)	1.98	643, 698	0.66, 0.31
	4%	7	774 (128.93 mA/cm^2)	3.58 (5.78 mA/cm^2)	1.72	645, 693	0.67, 0.31
	8%	8.3	1078 (231.14 mA/cm^2)	3.78 (1.94 mA/cm^2)	1.82	645, 695	0.67, 0.31
6c	1%	5.5	528 (140.99 mA/cm^2)	3.50 (0.59 mA/cm^2)	1.68	642, 698	0.65, 0.31
	2%	6	843 (238.90 mA/cm^2)	3.97 (0.53 mA/cm^2)	1.91	643, 693	0.66, 0.31
	4%	6.5	249 (13.43 mA/cm^2)	4.84 (1.19 mA/cm^2)	2.33	644, 694	0.66, 0.31
	8%	7.5	858 (107.92 mA/cm^2)	4.14 (4.76 mA/cm^2)	1.99	644, 693	0.65, 0.31
(Piq)Pt(acac)	1%	6	1471 (245.49 mA/cm^2)	3.92 (3.96 mA/cm^2)	1.88	598, 644	0.62, 0.36
	2%	6.5	1418 (232.15 mA/cm^2)	3.67 (6.14 mA/cm^2)	1.76	597, 645	0.63, 0.36
	4%	9	1041 (132.07 mA/cm^2)	3.39 (6.62 mA/cm^2)	1.63	597, 648	0.63, 0.35
	8%	9.6	844 (107.17 mA/cm^2)	2.68 (7.40 mA/cm^2)	1.29	599, 646	0.62, 0.35

and below the level of the PFO host (3.7 eV), the offsets in HOMO and LUMO energy levels between the Pt(II) complexes and PFO-PBD are available to promote charge trapping and direct exciton formation on the phosphorescent molecules [40].

The current density–voltage–luminance (*I*–*V*–*L*) curves of the **6a**-doped PLEDs at different doping concentrations are shown in Fig. 6. The devices exhibited low turn-on voltages of 5.5–8.0 V. The current density increased with increasing **6a** doping concentration from 1% to 2%, but decreased with increasing **6a** doping concentration from 2% to 8%. This implies that the energy transfer processes of the (Piq-G)Pt(acac)-doped devices are dominated by not only charge trapping process, but also the Förster energy transfer or Dexter transfer mechanism.

Table 4 summarized the device performances of the platinum (II) complexes-doped PLEDs at different dopant concentrations. In these devices, the diphenylamino-functionalized **6a**-doped devices exhibited the best device performance. A maximum brightness of 1501 cd m^{-2} at 75.03 mA cm^{-2} and a maximum EQE 8.6% at 0.66 mA cm^{-2} were obtained in the **6a**-doped device at 4% doped concentration (Fig. 6 inset). Compared with (Piq)Pt(acac), the diarylamino-functionalized (Piq-G)Pt(acac) complexes presented higher luminescent efficiency in the PLEDs. The luminescent efficiency of **6a**-doped devices is two times higher than that of (Piq)Pt (acac)-doped devices. This means that incorporation of diarylamino unit to the platinum (II) complexes can improve electroluminescent properties of the platinum (II) complexes. The nonplanar triphenylamino moiety in the platinum complexes has a potential to efficiently reduce π–π stacking and Pt–Pt interactions.

4. Conclusions

We have demonstrated the synthesis, optical and redox properties, as well as electrophosphorescence of a class of the diarylamino-functionalized platinum complexes. A maximum external quantum efficiency of 8.6% was obtained in a double-layer PLED using a diphenylamino-functionalized platinum complex as dopant at 4% doping concentration. All of these functionalized (Piq-G)Pt (acac) complexes exhibited better device performance than nonfunctionalized (Piq)Pt(acac) complex. The presented diarylamino-functionalized platinum complexes are promising organic phosphors in high-efficiency red-emitting PLEDs.

Acknowledgment

The authors would like to thank the National Natural Science Foundation of China (Project No. 20772101 and 50973053), Hunan Provincial Science Foundation (Project No. 2007FJ3017 and 2009FJ2002) Hunan Province Postgraduate Research and Innovation Foundation (projects No. S2008yjscx09) for financial support for this work.

Appendix. Supplementary material

CCDC 745886 contains the supplementary crystallographic data for this paper. This data can be obtained free of charge from The Cambridge Crystallographic Data Centre via http://www.ccdc.cam.ac.

References

[1] Peyratout CS, Aldridge TK, Crites DK, McMillin DR. DNA-binding studies of a bifunctional platinum complex that is a luminescent intercalator. Inorganic Chemistry 1995;34(17):4484–9.
[2] Wang AHJ, Nathans J, Van Der Marel GA, Van Boom JH, Rich A. Molecular structure of a double helical DNA fragment intercalator complex between deoxy CpG and a terpyridine platinum compound. Nature 1978;276:471–4.
[3] Houlding VH, Frank AJ. Cooperative excited-state behavior in platinum(II) Magnus-type double-salt materials. Active and inactive photosensitizers for hydrogen production in aqueous suspension. Inorganic Chemistry 1985;24 (22):3664–8.
[4] Maruyama T, Yamamoto T. Effective photocatalytic system based on chelating π-conjugated poly(2,2′-bipyridine-5,5′-diyl) and platinum for photoevolution of H_2 from aqueous media and spectroscopic analysis of the catalyst. Journal of Physical Chemistry B 1997;101(19):3806–10.
[5] Anbalagan V, Srivastava TS. Spectral and photochemical behaviour of mononuclear and dinuclear α-diimine complexes of Pt(II) and Pd(II) with catechol derivatives. Journal of Photochemistry and Photobiology A: Chemistry 1995;89(2):113–9.
[6] Roundhill DM, Gray HB, Che CM. Pyrophosphito-bridged diplatinum chemistry. Accounts of Chemical Research 1989;22(2):55–61.
[7] Nocera DG. Chemistry of the multielectron excited state. Accounts of Chemical Research 1995;28(5):209–17.
[8] Paw W, Cummings SD, Mansour MA, Connick WB, Geiger DK, Eisenberg R. Luminescent platinum complexes: tuning and using the excited state. Coordination Chemistry Reviews 1998;171(1):125–50.
[9] Hissler M, McGarrah JE, Connick WB, Geiger DK, Cummings SD, Eisenberg R. Platinum diimine complexes: towards a molecular photochemical device. Coordination Chemistry Reviews 2000;208(1):115–37.
[10] McGarrah JE, Kim YJ, Hissler M, Eisenberg R. Toward a Molecular Photochemical Device: a triad for photo induced charge separation based on a platinum diimine bis(acetylide) chromophore. Inorganic Chemistry 2001;40 (18):4510–1.

[11] James EM, Eisenberg R. Dyads for photo induced charge separation based on platinum diimine bis(acetylide) chromophores: synthesis, luminescence and transient absorption studies. Inorganic Chemistry 2003;42(14):4355–65.
[12] Baldo MA, O'Brien DF, You Y, Shoustikov A, Sibley S, Thompson ME, et al. Highly efficient phosphorescent emission from organic electroluminescent devices. Nature 1998;395:151–4.
[13] Kwong RC, Sibley S, Dubovoy T, Baldo MA, Forrest SR, Thompson ME. Efficient, saturated red organic light emitting devices based on phosphorescent platinum(II) porphyrins. Chemistry of Materials 1999;11(12):3709–13.
[14] Cleave V, Yahioglu G, Barny PL, Friend RH, Tessler N. Harvesting singlet and triplet energy in polymer LEDs. Advanced Materials 1999;11(4):285–8.
[15] Baldo MA, Lamansky S, Burrows PE, Thompson ME, Forrest SR. Very high-efficiency green organic light-emitting devices based on electrophosphorescence. Applied Physics Letters 1999;75(1):4–6.
[16] Cocchi M, Kalinowski J, Fattori V, Williams JAG, Murphy L. Color-variable highly efficient organic electrophosphorescent diodes manipulating molecular exciton and excimer emissions. Applied Physics Letters 2009;94(7):073309-1–073309-3.
[17] Cocchi M, Kalinowski J, Virgili D, Williams JAG. Excimer-based red/near-infrared organic light-emitting diodes with very high quantum efficiency. Applied Physics Letters 2008;92(11):113302-1–113302-3.
[18] Furuta PT, Deng L, Garon S, Thompson ME, Frchet JMJ. Platinum-functionalized random copolymers for use in solution-processible, efficient, near-White organic light-emitting diodes. Journal of the American Chemical Society 2004;126(47):15388–9.
[19] Kavitha JS, Chang Y, Chi Y, Yu JK, Hu YH, Chou PT, et al. In search of high-performance platinum(II) phosphorescent materials for the fabrication of red electroluminescent devices. Advanced Functional Materials 2005;15(2):223–9.
[20] Hu ZY, Luo CP, Wang L, Huang FL, Zhu KM, Wang YF, et al. Highly efficient saturated red electrophosphorescence from isoquinoline-based iridium complex containing triphenylamine units in polymer light-emitting devices. Chemical Physics Letters 2007;441(4–6):277–81.
[21] Xu ZW, Li Y, Ma XM, Gao XD, Tian H. Synthesis and properties of iridium complexes based 1,3,4-oxadiazoles derivatives. Tetrahedron 2008;64(8):1860–7.
[22] Xia ZY, Xiao Xiao X, Su JH, Chang CS, Chen CH, Li DL, et al. Low driving voltage and efficient orange-red phosphorescent organic light-emitting devices based on a benzotriazole iridium complex. Synthetic Metals 2009;159(17–18):1782–5.
[23] Wong WY, He Z, So SK, Tong KL, Lin ZY. A multifunctional platinum-based triplet emitter for OLED applications. Organometallics 2005;24(16):4079–82.
[24] Zhu WG, Liu J, Luo CP, Hu ZY, Zhu MX. Zhongguo Faming Zhuanli, ZL 200510032482.XA; 2005 (in Chinese).
[25] Liang B, Jiang CY, Chen Z, Zhang XJ, Shi HH, Cao Y. New iridium complex as high-efficiency red phosphorescent emitter in polymer light-emitting devices. Journal of Materials Chemistry 2006;16:1281–6.
[26] Patil NM, Kelkar AA, Nabi Z, Chaudhari RV. Novel CuI/tributyl phosphine catalyst system for amination of aryl chlorides. Chemical Communications 2003;19:2460–1.
[27] Cockburn BN, Howe DV, Keating T, Johnson BFG, Lewis J. Reactivity of co-ordinated ligands. Part XV. Formation of complexes containing Group V donor atoms and metal–carbon bonds. Journal of the Chemical Society Dalton Transactions 1973;4:404–10.
[28] Chassot L, Müller E, Von Zelewsky A. cis-Bis(2-phenylpyridine)platinum(II) (CBPPP): a simple molecular platinum compound. Inorganic Chemistry 1984;23(25):4249–53.
[29] Ghedini M, Pucci D, Crispini A, Barberio G. Oxidative addition to cyclometalated azobenzene platinum(II) complexes: a route to octahedral liquid crystalline materials. Organometallics 1999;18(11):2116–24.
[30] Lamansky S, Djurovich P, Murphy D, Abdel-Razzaq F, Kwong R, Tsyba I, et al. Synthesis and characterization of phosphorescent cyclometalated iridium complexes. Inorganic Chemistry 2001;40(7):1704–11.
[31] Lamansky S, Djurovich P, Murphy D, Abdel-Razzaq F, Lee HE, Adachi C, et al. Highly phosphorescent bis-cyclometalated iridium complexes: synthesis, photophysical characterization, and use in organic light emitting diodes. Journal of the American Chemical Society 2001;123(18):4304–12.
[32] Su YJ, Huang HL, Li CL, Chien CH, Tao YT, Chou PT, et al. Highly efficient red electrophosphorescent devices based on iridium isoquinoline complexes: remarkable external quantum efficiency over a wide range of current. Advanced Materials 2003;15(11):884–8.
[33] Colombo MG, Hauser A, Gudel HU. Evidence for strong mixing between the LC and MLCT excited states in bis(2-phenylpyridinato-C2, N')(2,2′-bipyridine) iridium(III). Inorganic Chemistry 1993;32(14):3088–92.
[34] Schmid B, Garces FO, Watts RJ. Synthesis and characterizations of cyclometalated iridium(III) solvento complexes. Inorganic Chemistry 1994;33 (1):9–14.
[35] Zhou GJ, Wong WY, Poon SY, Ye C, Lin ZY. Symmetric versus unsymmetric platinum(II) bis(aryleneethynylene)s with distinct electronic structures for optical power limiting/optical transparency trade-off optimization. Advanced Functional Materials 2009;19(4):531–44.
[36] Evans RC, Douglas P, Winscom CJ. Coordination complexes exhibiting room temperature phosphorescence: evaluation of their suitability as triplet emitters in organic light emitting diodes. Coordination Chemistry Reviews 2006;250(15–16):2093–126.
[37] He Z, Wong WY, Yu X, Kwok HS, Lin Z. Phosphorescent platinum(II) complexes derived from multifunctional chromophores: synthesis, structures, photophysics, and electroluminescence. Inorganic Chemistry 2006;45(26):10922–37.
[38] Bronstein HA, Finlayson CE, Kirov KR, Friend RH, Williams CK. Investigation into the phosphorescence of a series of regioisomeric iridium(III) complexes. Organometallics 2008;27(13):2980–9.
[39] Thelakkat M, Schmidt HW. Synthesis and properties of novel derivatives of 1,3,5-tris(diarylamino)benzenes for electroluminescent devices. Advanced Materials 1998;10(3):219–23.
[40] Baldo1 MA, Thompson ME, Forrest SR. Phosphorescent materials for application to organic light emitting devices. Pure and Applied Chemistry 1999;71 (11):2095–6.